X-BAND RF PHOTOINJECTOR FOR LASER COMPTON X-RAY AND GAMMA-RAY SOURCES*

R.A. Marsh[†], G.G. Anderson, S.G. Anderson, D.J. Gibson, C.P.J. Barty
Lawrence Livermore National Laboratory, Livermore, CA 94550, USA

Abstract

Extremely bright narrow bandwidth gamma-ray sources are expanding the application of accelerator technology and light sources in new directions. An X-band test station has been commissioned at LLNL to develop multi-bunch electron beams. This multi-bunch mode will have stringent requirements for the electron bunch properties including low emittance and energy spread, but across multiple bunches. The test station is a unique facility featuring a 200 MV/m 5.59 cell X-band photogun powered by a SLAC XL4 klystron driven by a Scandinova solid-state modulator. This paper focuses on its current status including the generation and initial characterization of first electron beam. Design and installation of the inverse-Compton scattering interaction region and upgrade paths will be discussed along with future applications.

INTRODUCTION

Accelerator-based x-ray and gamma-ray sources are expanding rapidly, with several large facilities in construction both in Japan and in Europe [1, 2]. LLNL has a successful history utilizing gamma-rays generated by a linac-driven, laser-based Compton scattering gamma-ray source [3, 4, 5, 6]. Next generation advancements in linac-based x-ray and gamma-ray production require increasing the average flux of gamma-rays at a specific energy (that is, $N/eV/sec$ at the energy of interest). One way to accomplish this is to increase the effective repetition rate by operating the RF photoinjector in a multi-bunch mode, accelerating multiple electron bunches per RF macro-pulse. This multi-bunch mode will have stringent requirements for the electron bunch properties including low emittance and energy spread, but across multiple bunches. An X-band test station has been built and commissioned at LLNL to develop multi-bunch electron beams and generate x-rays. This paper summarizes progress and describes the current status and future direction of the project.

Building on the design work for a 250 MeV gamma-ray source, and leveraging hardware and engineering done for the VELOCIRAPTOR X-band accelerator [7], LLNL established an X-band test station for laser-Compton research and development. The current test station parameters are summarized in Table 1. Beam dynamics are summarized in Fig. 1 for a 100 pC bunch generated in the Mark 1 X-band

RF gun and accelerated by a single T53 traveling wave accelerating section. The goals of establishing the test station have been a demonstration of X-band technology for laser-Compton applications and pushing the state-of-the-art with novel interaction concepts. The current goals of the test station efforts are first x-ray demonstration, initial x-ray application experiments, electron beam optimization, demonstration of multiple electron bunches spaced as close as every RF bucket, and upgraded controls systems. Success has been achieved on all of these fronts, with preliminary results reported in this paper and [8].

Table 1: Test Station Parameters

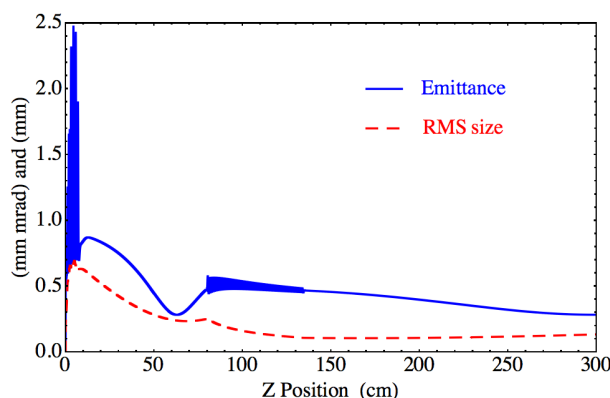|	
Charge	25–250 pC
Bunch Duration	2 ps
Bunch Rise/Fall	<250 fs
Normalized Emittance	<1 mm mrad
Gun Energy	7 MeV
Cathode Field	180–200 MV/m
Coupling β	1.7
Section Gradient	~70 MV/m
Final Energy	30 MeV

Figure 1: PARMELA beam dynamics simulation for a bunch charge of 100 pC.

TEST STATION

The accelerator is built around a state-of-the-art X-band RF photoinjector [9]. RF power is provided by a 50 MW 11.424 GHz SLAC built XL4 klystron powered by a solid-state Scandinova modulator. The high voltage modulator

and X-band tube reside in a separate area with RF distribution fed through a hole in the wall to the linear accelerator. A manifold divides the power between the RF gun and the accelerating sections. The RF power provided is of very high phase and power stability, providing excellent electron beam consistency. A 5.59 cell RF gun incorporates LCLS S-band gun improvements, producing 7 MeV submicron emittance bunches in excess of 100 pC. A SLAC designed T53 traveling wave accelerating section is used to boost the energy from 7 MeV to a maximum of up to 31 MeV. The T53VG3MC is a traveling wave section with a group velocity of 3 percent of the speed of light, with mode converter couplers [10]. The mode converter couplers on these section have been redesigned to incorporate an RF dipole and quadrupole canceling racetrack shape. A second T53 accelerating section will be installed to further increase the energy reach of the test station. Beam steering uses X-Y windowpane dipole magnets. Two quadrupole triplets focus the beam for transport, final focus for the laser interaction, and are used for quad-scan emittance measurement. A chicane is used to shield x-ray experiments from dark current and allow for an interaction laser exit path. The electron beam energy is measured with a dipole magnet that has been calibrated to serve as a spectrometer, and captured in a shielded dump. Other diagnostics include ICTs, YAG screens, and OTR measurements.
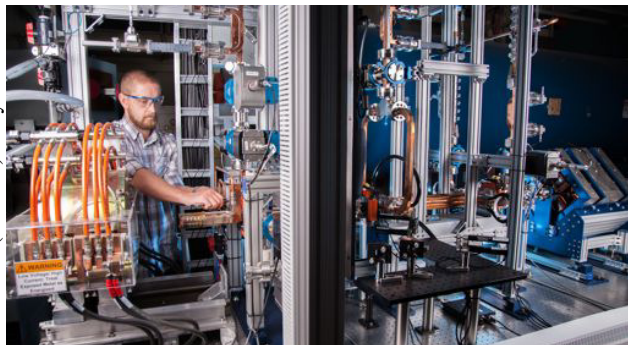

Figure 2: Photograph of the X-band test station.

Laser

There are two laser systems involved in the x-ray generation system at LLNL. The first is the Photocathode Drive Laser, which generates the electron beam. It is a chirped pulse amplification system, based on Ti:Sapphire that is shared with the main S-band 100 MeV accelerator facility. This laser provides up to 20 mJ of uncompressed 780 nm laser light which is transported to the accelerator, where a dedicated compressor and frequency tripler compresses the pulse to 200 fs. The beam is then apertured to provide a sharp radial edge, typically with a 0.5 mm diameter. The apertured beam is then relay imaged to the photoinjector cathode, providing typically 10 μJ per pulse in the UV. In order to generate multiple pulses, a hyper-Michelson pulse stacker [11] is used. The second laser is a commercial frequency doubled Nd:YAG laser that produces up to 800 mJ

of 532 nm light in a 6 ns pulse. The ideal laser would be a few-ps long laser pulse, which would increase the total x-ray flux by a couple orders of magnitude. We have demonstrated such a system in the past, but havent integrated it into the X-band test station. For the current work underway, the commercial system in place is sufficient.

Interaction Region

The final accelerated beam is diverted from and returned to the main beam axis by a magnetic chicane. This allows us to both shield the downstream x-ray diagnostic from on-axis dark current bremsstrahlung noise in the high-gradient components as well as collect the laser light after the scattering interaction. The beam is then focused to a <50 μm spot by a quadrupole triplet, at which point it interacts with the laser. After the interaction, the beam is diverted from the x-ray path with a dipole that doubles as a spectrometer and the beam is then dumped in a carbon block. The current interaction laser is a 6 ns, 800 mJ, 10 Hz, 532 nm commercial Nd:YAG laser system that will eventually be replaced by a 120 Hz, 1 J, 10 ps laser system to significantly increase the x-ray flux. The laser beam is focused to a 50 μm rms spot with a 1 m focal length lens, passing though the spectrometer dipole as well as one of the chicane dipoles before being collected and dumped. A more detailed explanation of the laser systems and interaction region is available in [8].

RESULTS

The commissioning of the test station took place in stages: initial testing of the high voltage modulator and klystron [12], RF conditioning of the T53 section to 25 MW and 200 ns, RF conditioning of the Mark 1 RF gun to 200 MV/m gradient, and finally electron beam production and characterization. Arc detection is active on the klystron forward and reverse power, as well as the RF gun and accelerator section reverse power traces. Initially arc detection was by fixed threshold comparison, but this system has been supplanted by a fast comparator architecture where an arc is identified as too large a deviation of the current trace from the previous one.

First beam was observed on the initial phase scan with photocathode laser illumination, attributed to precision alignment of the beamline components. Relatively high quantum efficiencies have been observed for the copper photocathode, $\sim 2 \times 10^{-5}$. Rough tuning has resulted in energy spread on order 0.1% at up to 31 MeV, limited by available RF power. Quadrupole scans have been performed and are currently accomplished using integrated controls software for data acquisition, image analysis, and beam envelope equation fitting for final emittance. This improvement in controls has enabled rapid tuning of the machine, resulting in emittances within a factor of 2 of PARMELA beam dynamics predictions. Further tuning and optimization of laser parameters is underway and lowering this margin continually.
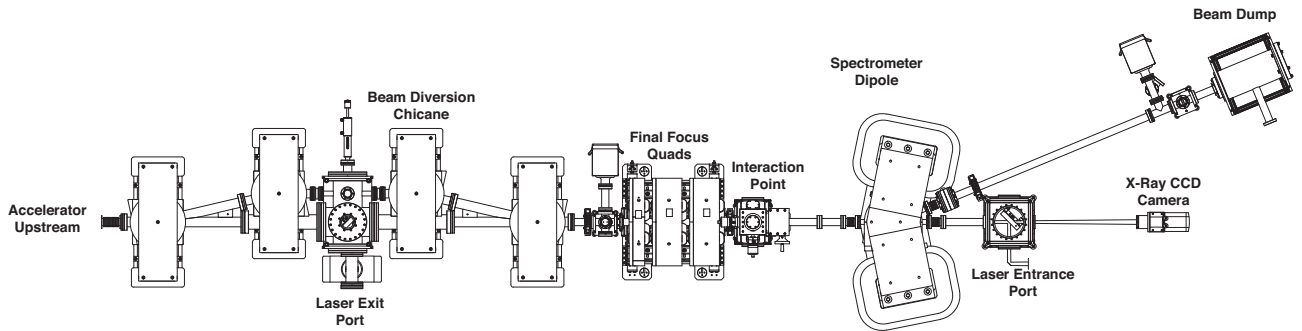
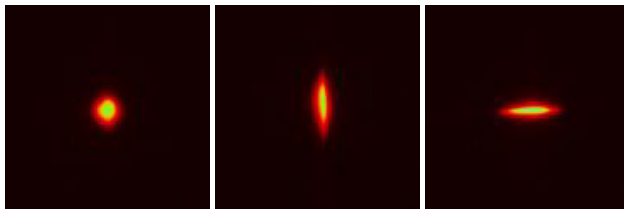Figure 3: Schematic of interaction point as built.

Figure 4: Beam images on YAG screen for quad scan: unfocused, focused in X, and focused in Y.

Electron beam optimization is the focus of current efforts, both to achieve the lowest emittance possible and to establish the scaling of emittance with charge in order to determine the optimum electron beam parameters for x-ray production on the test station. Current results show linear scaling of emittance with charge, prompting investigation of lower charge and emittance bunches. In addition, retuning of the machine for the highest possible charge is being investigated for x-ray applications insensitive to bandwidth.

The emittance of multiple simultaneous bunches is also currently being measured. Preliminary results show no significant degradation of performance between single-bunch and multiple-bunch operation. Beam dynamics modeling is underway to distinguish the effect of bunch-to-bunch emittance growth and statistical variation in the images used for the quad scan parameter fitting. Ultimately, streaked OTR-based quadrupole scans will be able to simultaneously measure the emittance of each bunch, and confirm operation of laser-Compton sources in multibunch modes.

First electron beam has been followed by first x-ray beam a year later. New interaction laser optics and realignment of the x-ray camera have produced excellent x-ray results, with precision calibration to determine how close the photon flux matches predictions planned for this summer. More x-ray results are presented in [8].

CONCLUSION

The LLNL laser-Compton source is operational and now offers a valuable test bed to optimize all areas of source development. Great initial success in producing laser-Compton x-rays, and using multiple bunches to increase x-ray flux are an important first step in increasing photon flux. The electron beam is being further optimized, and charge scaling is being compared to modeling to optimize both this system and electron sources for different laser-Compton interaction geometries. Multi-bunch electron beam measurements are being made and compared to modeling to confirm bunch-to-bunch effects. The controls system for the test station is currently being upgraded to make operation of the accelerator easier and more robust. Significant next steps involve full implementation of multi-GHz lasers systems to take full advantage of higher flux generation, as well as facility upgrades to increase the electron beam energy and thus the energy of the laser-Compton produced x-rays.

REFERENCES

[1] *Nuclear Physics and Gamma-ray Sources for Nuclear Security and Nonproliferation*, World Scientific Publishing Co. Ltd., Singapore (2015).

[2] *Technical Design Report EuroGammaS proposal for the ELI-NP Gamma beam System*, http://arxiv.org/abs/1407.3669 (2014).

[3] C.P.J. Barty, and F.V. Hartemann, *"T-REX: Thomson-Radiated Extreme X-rays Moving X-ray Science into the "Nuclear" Applications Space with Thomson Scattered Photons"*, **UCRL-TR-206825** (2004).

[4] F. Albert, *et al.*, Opt. Lett. **35**, 354 (2010).

[5] D.J. Gibson, *et al.*, Phys. Rev. STAB **13**, 070703 (2010).

[6] F. Albert, *et al.*, Phys. Rev. STAB **13**, 070704 (2010).

[7] S.G. Anderson, *et al.*, Nucl. Instrum. Methods Phys. Res., Sect. A, **657** 1, pp. 140–149 (2011).

[8] D.G. Gibson, *et al.*, *This conference*, **TUBC2** IPAC 2015.

[9] R.A. Marsh, *et al.*, Phys. Rev. ST Accel. Beams, **15**, 102001 (2012).

[10] C. Adolphsen, **ROPC006**, PAC 2003.

[11] C.W. Siders, et al., Appl. Opt. **37**, 5302 (1998).

[12] R.A. Marsh, *et al.*, Nucl. Instrum. Methods Phys. Res., Sect. A, *in preparation* (2013).